

# **AUTOMATIC GUIDANCE OF AGRICULTURAL VEHICLES AT HIGH FIELD SPEEDS**

by

**T. S. Stombaugh**

Assistant Professor  
Food, Agricultural and Biological Engineering  
The Ohio State University  
Columbus, OH

**E. R. Benson**

Graduate Fellow  
Agricultural Engineering  
Univ. of Illinois at Urbana-Champaign  
Urbana, IL

**J. W. Hummel**

Agricultural Engineer  
USDA - Agricultural Research Service  
Urbana, IL

Written for Presentation at the  
1998 ASAE Annual International Meeting  
Sponsored by ASAE

Disney's Coronado Springs Resort  
Orlando, FL  
July 12-16, 1998

## **Summary:**

An automatic steering controller was installed on a Case-IH Model 7220 tractor. The primary posture sensor was a kinematic differential GPS. Open loop and closed loop frequency response tests were conducted to evaluate the steering controller dynamics. A double integrator transfer function adequately related vehicle lateral deviation to steering angle within the frequency range of 0.04 Hz to 0.5 Hz. Forward placement of the posture sensor was critical to reducing the phase lag, allowing the use of a simplified guidance controller design.

## **Keywords:**

Automatic Guidance, Controls, GPS, Vehicle Dynamics

The author(s) is solely responsible for the content of this technical presentation. The technical presentation does not necessarily reflect the official position of ASAE, and its printing and distribution does not constitute an endorsement of views which may be expressed.

Technical presentations are not subject to the formal peer review process by ASAE editorial committees; therefore, they are not to be presented as refereed publications.

Quotation from this work should state that it is from a presentation made by (name of author) at the (listed) ASAE meeting.

EXAMPLE — From Author's Last Name, Initials. "Title of Presentation." Presented at the Date and Title of meeting, Paper No X. ASAE, 2950 Niles Road, St. Joseph, MI 49085-9659 USA.

For information about securing permission to reprint or reproduce a technical presentation, please address inquiries to ASAE.

## INTRODUCTION

Over the past century, many changes have occurred in agricultural field production machinery. The general trend has been toward bigger and faster machines, allowing operators to finish field operations faster and ultimately cover more field area. Most agricultural field operations are performed using parallel swathing or switchback operation (Grovmum and Zoerb, 1970). This kind of operation is very repetitive and can become monotonous for the operator. Although the tendency toward bigger and faster machinery has made it possible to complete field operations faster and with fewer trips, the basic parallel swathing pattern has not changed. In fact, manual guidance has become more difficult because of the skill required to navigate the larger equipment at higher speeds.

A land vehicle guidance system can be conceptualized by the signal flow diagram shown in Figure 1. The posture of a vehicle is the position and orientation of a vehicle relative to some reference frame (Kanayama and Hartman, 1989). In simplest terms, a guidance system determines the current posture of a vehicle, compares it to a desired posture, and executes appropriate steering control to direct the vehicle toward the desired posture.

Manual operator steering control follows this same concept. A desired path is determined by the operator, usually from visual cues such as stationary objects at the edge of the field, previous swaths, or some kind of deliberately placed guidance marks (foam blobs, guidance furrows, etc.). The operator observes the current posture of the vehicle and makes appropriate steering adjustments through the steering wheel.

Automated guidance systems attempt to relieve the operator from many, if not all, of the tasks involved in guiding a vehicle. One major benefit of automatic guidance systems is a reduction in machine operator fatigue by automating repetitively monotonous steering tasks.

Another benefit of automatic guidance systems is a potential improvement in the placement of agricultural inputs. With larger equipment, human operators often overlap previous paths in field operations, subjecting parts of a field to a double application of farming inputs (Nieminen and Sampo, 1993). An automatic guidance system can control the path of larger vehicles, such as chemical application equipment, more precisely than a human operator can, thus reducing the amount of treatment overlap.

Furthermore, the agriculture industry is experiencing a fundamental change in field management practices. Site-specific crop management technology and associated equipment allow farmers to apply inputs only where needed and at the necessary rates. Automatic guidance systems will become an integral part of the precision placement system, freeing the operator to monitor variable rate control equipment.

The purpose of this study was to implement an automatic guidance system on an agricultural vehicle. Specific study topics were the dynamics of an agricultural tractor traveling at speeds exceeding 4.5 m/s and the possibility of achieving adequate

guidance control using only a Global Positioning System (GPS) receiver for position sensing.

## REVIEW OF LITERATURE

Significant research efforts have focused on development of feedback controllers for automatic vehicle guidance. Researchers who employed a model-based approach to controller design first developed a mathematical model of tractor dynamics. A theoretical feedback controller was then developed to properly control the mathematical model, and field tests were used to verify and fine-tune the controller. Erbach et al. (1991) stated that for the modeled approach to work, the frictional characteristics between the vehicle tire and soil surface must be small or at least constant. Since friction is neither negligible nor constant, cornering forces can produce significant and unpredictable sideslip. Erbach et al. (1991) also claimed that under normal field conditions and especially at low speeds, cornering forces are small, rendering sideslip negligible and vehicle dynamics models valid.

Choi et al. (1990) developed the following system of discrete-time equations to describe the motion of an agricultural tractor:

$$\begin{aligned}
 Fx_{(k+1)} &= d \cos\left(\frac{d\alpha_r}{2} + \delta_{(k)} + \Psi_{(k)}\right) + Fx_{(k)} \\
 Fy_{(k+1)} &= d \sin\left(\frac{d\alpha_r}{2} + \delta_{(k)} + \Psi_{(k)}\right) + Fy_{(k)} \\
 \Psi_{(k+1)} &= \frac{d}{L} \left(\frac{d\alpha_r}{2} + \delta_{(k)}\right) + \Psi_{(k)} \\
 lx_{(k+1)} &= Fx_{(k+1)} - h \cos(\Psi_{(k+1)}) \\
 ly_{(k+1)} &= Fy_{(k+1)} - h \sin(\Psi_{(k+1)})
 \end{aligned} \tag{1}$$

More recently, O'Connor et al. (1996) developed a steering controller based on the following set of linearized equations of motion:

$$\begin{aligned}
 \dot{y} &= V\Psi + \frac{VL_2}{L} \delta \\
 \dot{\Psi} &= \frac{V}{L} \delta \\
 \dot{\delta} &= u
 \end{aligned} \tag{2}$$

Both models (Equations 1 and 2) are kinematic models. Both research teams assumed that the wheels of the vehicle would not experience any sideslip. This assumption allowed them to base the model solely on the geometric properties of the vehicle while ignoring all mass and inertial properties. The major limitation of their subsequent controller designs is that operation was limited to slower forward vehicle speeds.

Obviously as vehicle forward speed increases, tire sideslip during turning maneuvers also increases, rendering kinematic models inadequate.

One of the most common dynamic models used to describe vehicle behavior is the bicycle model. Alleyne and DePoorter (1997) used the following version of the bicycle model to describe automobile dynamics:

$$\frac{y(s)}{\delta(s)} = \frac{C_{sf} V^2 (m L_1 d_s + I_{zz}) s^2 + C_{sf} C_{sr} L V (d_s + L_2) s + C_{sf} C_{sr} L V^2}{s^2 [I_{zz} m V^2 s^2 + V (I_{zz} (C_{sf} + C_{sr}) + m (C_{sf} L_1^2 + C_{sr} L_2^2)) s + (m V^2 (C_{sr} L_2 - C_{sf} L_1) + C_{sf} C_{sr} L^2)]} \quad (3)$$

This model has one input (steering angle) and one output (lateral position). Though this is a dynamic model including tire sideslip effects, the researchers still assumed that lateral tire forces are proportional to the sideslip angle, or the angle between the centerline of the tire and the actual direction of motion, and that forward speed is constant.

## OBJECTIVES

The main objective of this project was to design an automated agricultural vehicle guidance system capable of controlling the vehicle under higher speed agricultural conditions (exceeding 4.5 m/s).

The following subobjectives were established for this project:

1. Identify and verify a suitable mathematical model structure to describe the high speed dynamics of an agricultural tractor.
2. Design and test a robust guidance controller capable of providing guidance of an agricultural vehicle at speeds exceeding 4.5 m/s under controlled operating conditions that might be encountered on Midwestern grain farms.
3. Identify model/controller features that preclude universal application of the concept.

## EQUIPMENT AND PROCEDURES

To complete the previously stated objectives, the following procedures were implemented. First, an agricultural vehicle (Case-IH Magnum Model 7220<sup>1</sup> two-wheel-drive farm tractor) was instrumented with an automatic steering controller and posture sensors. The tractor had a mass of 8120 kg and had an estimated yaw moment of inertia of 23,000 kg-m<sup>2</sup> according to data provided by Case Corporation. The tests were conducted with three standard wheel weights on each rear wheel and no extra weights on the front end, yielding front and rear axle masses of 2155 kg and 5965 kg, respectively. This weight configuration was chosen to minimize rear wheel side-slip and allow some front wheel side-slip during cornering maneuvers while not deviating significantly from typical operating configurations. Tractor forward velocity was varied by changing transmission gear while operating the engine at a constant 2200 rpm.

The configuration of the automatic steering controller (Figure 2) included a linear potentiometer wheel angle sensor, which was mounted rigidly to the steering cylinder of the tractor. The actuating rod of the sensor was connected to the tractor frame with a tongue-in-slot mechanism to protect the sensor from misalignment and steering cylinder flexure. Calibration tests indicated a linear relationship between sensor output and steering wheel angle (Stombaugh, 1998).

The steering valve was an experimental electrohydraulic proportional valve provided by Case Corporation. The valve was plumbed in parallel with the existing steering hand pump. When activated, the automated valve overrode manual steering inputs, but did not interfere with manual steering when not activated. The electrohydraulic valve required a pulse-width-modulated (PWM) signal for proportional control. A commercial dual-coil valve driver was used to convert an analog DC voltage to an appropriate PWM signal. Feedback control was provided by a 9 MHz single-board microcontroller.

The primary posture sensor utilized for this project was a Novatel RT-20 Kinematic Differential GPS. A base station was installed and maintained at the University of Illinois Agricultural Engineering Research Farm, Urbana, IL, where most tests were conducted. The antenna of the rover GPS unit was initially mounted on top of the tractor cab over the vehicle center of gravity (c.g.). The GPS system manufacturer specified 20 cm accuracy (based on circular error probable) with maximum update rates of 5 Hz. Differential corrections were transmitted from the base station to the rover via a 9600 Baud radio modem.

The 150 MHz Pentium-based guidance computer was responsible for reading posture sensor outputs, computing and sending the appropriate steering commands to the steering controller, and logging any pertinent data. Additional serial ports were installed in the computer to facilitate communications with sensors and the steering controller.

---

<sup>1</sup> Mention of a trade name, proprietary product, or specific equipment does not constitute a guarantee or warranty by The Ohio State University, the University of Illinois, or the USDA - Agricultural Research Service and does not imply the approval of the named product to the exclusion of other products that may be suitable.

When weather permitted, field tests were conducted on a soil surface at the University of Illinois Agricultural Engineering Research Farm. A fallow, 26 m by 225 m east-west oriented plot was used for guidance work. The soils in the field were of the Drummer silty clay loam (Fine-silty, mixed, mesic Typic Haplaquolls) and Brenton silt loam (Fine-silty, mixed, mesic Aquic Argiudolls) series (Table 1). The plot was tilled after each set of tests with a cultimulcher to maintain a soft, yet relatively level and uniform surface. The field was periodically tilled with a subsoiler to a depth of about 0.3 m to prevent hard pan formation and to improve infiltration.

After the tractor was properly instrumented, *open loop frequency response* tests were conducted to quantify vehicle dynamic performance. Time-based sinusoidal steering commands of varying frequencies were generated by the guidance computer and sent to the steering controller. The actual wheel position was echoed back to the guidance computer from the steering controller. The guidance computer recorded the actual wheel angle as well as vehicle lateral response as indicated by the GPS. Tests were conducted at speeds of 2.6 and 4.5 m/s. Bode plots and transfer functions of the vehicle response were generated.

These preliminary open loop frequency response results were then used to design a guidance controller. The performance of this *preliminary guidance controller* was evaluated with step response tests.

Once the preliminary guidance controller was in place, more refined *closed loop frequency response* tests were performed. The sinusoidal inputs for the open loop frequency response tests were purely time based and not spatially referenced. As a result, it was sometimes difficult to keep the tractor within field boundaries, especially at higher speeds. Using the preliminary feedback controller, a spatially referenced input was generated and executed. Again, the guidance controller recorded the actual wheel

Table 1. Description of soils<sup>1</sup> in test plot.

	Drummer	Brenton
Surface soil		
Texture	Silty clay loam	Silt loam
Slope range	0 - 2 %	0 - 3 %
Thickness	38 cm	38 cm
Avg. organic matter content	6.0 %	4.5 %
Subsoil		
Texture	Silty clay loam	Silty clay loam-clay loam
Thickness	84 cm	84 cm
Natural drainage	Poorly drained	Somewhat poorly drained
Permeability	Moderate	Moderate

<sup>1</sup>Fehrenbacher, J.B., J.D. Alexander, I.J. Jansen, R.G. Darmody, R.A. Pope, M.A. Flock, E.E. Voss, J.W. Scott, W.F. Andrews and L.J. Bushue. 1984. Soils of Illinois. Agri. Expt. Sta. Bull. 778, Univ. of Ill. at Urbana-Champaign, Urbana IL.

angle and vehicle lateral motion. These data were used to refine the guidance controller. The controller was once again tested with vehicle step responses.

Further refinements in guidance controller design were achieved by quantifying and modifying the *steering controller dynamics*. Vehicle system models were verified with experimental data.

Finally, a short series of tests were conducted to evaluate the effects of fore-aft *GPS antenna location* on the controllability of the vehicle.

## RESULTS AND DISCUSSION

### *Open Loop Frequency Response*

Open loop frequency response tests were used to explore vehicle dynamics. An algorithm was implemented on the guidance computer to generate a time-based sinusoidal steering excitation and send it to the steering controller. The tractor was operated at a fixed velocity across the test field as the steering controller executed the sinusoidal commands and returned the actual wheel angle to the guidance computer. The guidance computer simultaneously recorded time, vehicle position and actual wheel angle data. Tests were conducted at 2.6 and 4.5 m/s. Steering input frequency was varied from 0.04 Hz to 0.4 Hz.

The measured wheel angle and vehicle lateral deviation as functions of time for a typical 0.1 Hz open loop frequency response test (Figure 3) show that the lateral response of the vehicle contained a sinusoidal component at the excitation frequency. The general path of the vehicle, neglecting the sinusoidal component, was not linear. Since the tests were truly open loop (i.e. no position feedback or control), a slight misalignment of the vehicle at the beginning of the test and asymmetries in the steering valve and controller caused the tractor to slowly veer out of the test area. This lateral drift limited the bandwidth of tests that could be conducted. Tests were also limited by field size since lower frequencies produced larger lateral deviations.

Assuming that the actual vehicle dynamics information was represented solely by the sinusoidal portion of the path, a search algorithm was written to extract the sinusoidal information from lateral position and wheel angle responses. For each response, the algorithm subtracted the mean value from the data to eliminate the DC component of the response. The algorithm then performed a search to find the amplitude and phase angle of the sinusoid, based on the least sum of squared errors.

The frequency responses for the two test speeds (Figure 4) exhibited a relatively linear response at a slope of -2 decades/decade. The gain, which related the lateral response of the vehicle to the actual steering angle, could be represented by the transfer function of the form:

$$H(s) = \frac{y(s)}{\delta(s)} = \frac{c}{s^2}. \quad (4)$$

Equation 4 is similar to the bicycle model (Equation 3) except that the bicycle model shows two additional higher frequency pole-zero pairs. Calculations based on the visually best fit lines in Figure 4 (ignoring apparent low frequency outliers) showed that  $c$  (Equation 4) was approximately 0.04 at 2.6 m/s and 0.1 at 4.5 m/s.

There was some apparent non-linearity in the frequency response data occurring just above 0.2 Hz. This non-linearity could have been caused by vehicle dynamics described by the pole-zero pairs in Equation 3. The non-linearity may also have resulted from measurement errors caused by the open loop nature of the preliminary tests. Aliasing is another possible source of measurement error since the maximum sampling frequency of the GPS sensor was 5 Hz. From the similarity of the shapes of the two data sets (Figure 4), it can be concluded that under limited conditions, an increase in velocity can be represented solely by an increase in the numerator constant,  $c$ , of the transfer function (Equation 4).

#### *Preliminary Guidance Controller*

A preliminary guidance controller was designed based on the model information obtained from Figure 4. Since the GPS antenna, which was mounted above the vehicle c.g., was behind the vehicle control point (front wheels), excessive phase lag precluded simple controller design. Therefore, the antenna was mounted 3 m above the ground on a pole extending upward from the front weight bracket 45 cm ahead of the front axle. A digitally implemented lead controller of the form:

$$C(s) = K \frac{s + 0.5}{s + 20} \quad (5)$$

provided stable performance (Figure 5). Though performance was stable, it was underdamped and contained a significant amount of steady state error.

#### *Closed Loop Frequency Response*

The preliminary guidance controller, though marginally effective, allowed more refined frequency response tests to be performed on the tractor system. The GPS sensor remained on the front of the tractor throughout the next several tests. A relatively simple control algorithm was developed to guide the tractor along sinusoidal paths varying about a given latitude. The amplitude of the sinusoid was varied to produce a reasonable output amplitude while not breaching the capabilities of the marginal guidance controller. Again, time, vehicle position and actual wheel angle were simultaneously recorded.

The Bode plots of these results (Figure 6) for tests at 4.5 and 5.1 m/s show that the general trends were very similar to the results of the open loop tests (Figure 4). The gain was nearly linear with a slope of -2 decades/decade, and the phase was approximately  $-180^\circ$  to a frequency of about 0.4 Hz. Again, there appeared to be some more complicated dynamics above 0.4 Hz. This trend agreed with results shown by DePoorter (1995) for automobiles and may be associated with the additional pole-zero

pairs defined by Equation 3. Because the dynamics in question were so near bandwidth limit, it was still difficult to draw any quantitative conclusions. Hence, vehicle dynamics were again assumed to follow Equation 4. The values of  $c$  for tests at 4.5 and 5.1 m/s tests were found to be 0.135 and 0.177, respectively.

### *Steering Controller Dynamics*

During the design of the preliminary guidance controller, the dynamics of the steering actuator (Figure 2) were ignored. To complete modeling efforts, frequency response tests were performed on the steering system alone. Bode plots for the steering controller (Figure 7) show that there was some resonant behavior occurring at a frequency of 0.6 Hz. An attempt was made to find a model that would describe this behavior. The best model of reasonable order was:

$$D(s) = \frac{\left(\frac{s}{3.2} + 1\right)^2}{\left(\frac{s}{1.16} + 1\right) \left(\left(\frac{s}{4.15}\right)^2 + \frac{2(0.395)}{4.15}s + 1\right)} \quad (6)$$

The solid lines (Figure 7) show the theoretical frequency response of Equation 6. The actual gain performance was accurately represented by Equation 6. The phase was not as well represented, but the general shape was similar. The phase offset was probably due to latency in wheel angle measurement or dead band characteristics of the steering valve.

The steering controller transfer function (Equation 6) was then considered in the simulations (Figure 8). A portion of the system root locus including vehicle (Equation 4), guidance controller (Equation 5) and steering controller (Equation 6) dynamics (Figure 9) shows that two of the steering controller poles become unstable at higher gain. It was previously shown that increasing forward velocity increases  $c$  (Figure 5); hence, as velocity increased, the overall system gain increased, and the steering controller poles were pushed into the right-half plane of the root locus plot, causing instability.

Results of a step response simulation that included the steering controller dynamics were compared to the experimental test results (Figure 10). Since the simulations accurately predicted the trends of the actual performance, it can be concluded that the form of the transfer functions for all identified components of the system (Equations 4, 5, and 6) were adequate.

The analog output of the microcontroller used to control the steering actuator (Figure 2) was very unstable and susceptible to electromagnetic interference. This instability hampered further refinement of the guidance controller. To overcome this limitation, the microcontroller and feedback control were removed from the steering controller scheme, and the steering actuator (Figure 2) was operated as an open loop component of the guidance system. Formerly, the input to the steering controller was the desired wheel

angle. After elimination of the feedback loop, the input to the steering actuator, in steady state, was proportional to the desired steering rate. An analog output from a data acquisition card in the guidance computer was used to control the PWM valve driver.

The steering actuator dynamics were measured with frequency response tests of the closed loop steering controller with simple proportional feedback parameters. The measured frequency response of the steering controller (Figure 11) showed that the closed loop system was second order and could be modeled as:

$$D(s) = \frac{1}{\left(\frac{s}{1.38} + 1\right)\left(\frac{s}{10} + 1\right)}. \quad (7)$$

The offset between the theoretical and experimental phase data (Figure 11) was attributed to time errors in experimental measurements and steering valve dead band compensation. The open loop dynamics of the steering actuator were then calculated to be:

$$G(s) = \frac{13.8}{s(s + 11.4)}. \quad (8)$$

A guidance controller of the form:

$$C(s) = \frac{u(s)}{e(s)} = K(s + 1)(s + 0.5) \quad (9)$$

provided good system performance in simulation. The feedback control described in Equation 9 is typically very difficult to implement since it is a pure second order differentiator, which will amplify high frequency noise. Since the sampling rate during field tests was relatively low (5 Hz), data were naturally filtered, and the controller was directly implemented digitally as:

$$u_{(k)} = K(ae_{(k)} - be_{(k-1)} + ce_{(k-2)}) = K(33e_{(k)} - 57.5e_{(k-1)} + 25e_{(k-2)}). \quad (10)$$

Field step response tests of the new controller were performed on both soil and asphalt surfaces. Step response results (Figure 12) showed that, as expected, more noise was present in soil tests than in asphalt tests. Any roll of the vehicle due to uneven surface conditions caused significant lateral motion of the antenna without an actual translation of the vehicle frame, since the GPS antenna was mounted to the tractor 3 m above the ground surface.

In general, system performance was improved over previous tests (Figure 5). The response with the new controller (Figure 12) settled to the final value much quicker and there was less overshoot as compared to preliminary guidance controller performance

(Figure 5). There was still significant steady state error present in the output. There was also a two to three second delay before the step response was seen on the output.

Since both the vehicle and steering actuator transfer functions (Equations 4 and 8) contain free integrators, the steady state error and time delay was attributed to a non-linearity in the system. Experimentation showed that steering actuator dead band contributed to the steady state error. When the voltage width for dead band compensation was set too narrow in the control algorithm (undercompensation), steady state error was introduced. When the width of the dead band compensation was increased to ensure there would be a significant flow response at both dead band boundaries, the steady state error and time delay in the start of the step response was eliminated (Figure 13, 4.5 m/s). Straight-line tests of vehicle response showed that the lateral position error at 4.5 m/s was within 16 cm (95% confidence).

Step response tests at increased speeds (Figure 13) showed a marked increase in noise of the output. Tire dynamics contributed to this noise by causing vehicle roll and thus, GPS antenna lateral deviation. The increase in system gain at higher speeds also contributed to the noisy output by causing the differentiating controller to amplify disturbances.

#### *GPS Antenna Location*

A brief series of tests were conducted to determine vehicle controllability with the GPS antenna mounted over the vehicle c.g. The previously designed guidance controller alone could not stabilize the system due to excessive phase lag. The GPS output was digitally integrated before feeding it into the guidance controller. This integration added enough phase lead to bring stability, but performance was still very oscillatory (Figure 14). Additional phase lead from supplemental sensors or a different guidance controller would be required to make the system performance acceptable with this sensor location.

## CONCLUSIONS

1. A double integrator transfer function can adequately relate vehicle lateral deviation to steering angle for a Case-IH Magnum Model 7220 two-wheel-drive tractor within the frequency range of 0.04 Hz to 0.5 Hz. Variations in tractor forward velocity (1.92 m/s to 6.8 m/s) affect only the numerator constant of the transfer function of this system.
2. A classical model-based guidance controller can provide adequate guidance system performance at forward velocities up to 6.8 m/s. Kinematic DGPS posture sensors should provide adequate guidance control for conditions similar to those included in these tests.
3. Placement of the posture sensor ahead of the vehicle control point is critical to reducing the phase lag, allowing the use of a simplified guidance controller design.

4. When automatic steering equipment dynamics and desired vehicle dynamics are in the same frequency range, the guidance controller design must compensate for both vehicle and steering equipment dynamics.
5. The dead band characteristic of the steering valve control is critical to guidance system performance. When dead band compensation is too narrow, the guidance system will exhibit significant steady state error.
6. A relatively slow update rate (5 Hz) of the GPS sensor results in natural filtering, and allows the use of a relatively unorthodox second-order derivative guidance controller. However, at this low sampling rate, higher frequency vehicle dynamics are not quantifiable.

## REFERENCES

- Alleyne, A. and M. DePoorter. 1997. Lateral displacement sensor placement and forward velocity effects on stability of lateral control of vehicles. Paper presented at the *American Controls Conference*. Albuquerque, NM, June 4-6.
- Choi, C. H., D. C. Erbach and R. J. Smith. 1990. Navigational tractor guidance system. *Transactions of the ASAE* 33(3):699-706.
- DePoorter, M. C. 1995. Development, experimentation, and control of a small scale vehicle dynamics and control laboratory. M.S. thesis. Library, University of Illinois at Urbana-Champaign, Urbana, IL.
- Erbach, T. C., C. H. Choi and K. Noh. 1991. Automated guidance for agricultural tractors. In *Proc. Automated Agriculture for the 21st Century*, ASAE Publication No. 11-91:182-191. St. Joseph, MI: ASAE.
- Grovum, M. A and G. C. Zoerb. 1970. An automatic guidance system for farm tractors. *Transactions of the ASAE* 13(5):565-573,576.
- Kanayama, Y. and B. I. Hartman. 1989. Smooth Local Path Planning for Autonomous Vehicles. In *Proc. IEEE International Conference on Robotics and Automation*, 3:1265-1270. Piscataway, NJ: IEEE.
- Nieminen, T. and M. Sampo. 1993. Unmanned vehicles for agricultural and off-highway applications. SAE Technical Paper Series No. 932475. Warrendale, PA: SAE.
- O'Connor, M., T. Bell, G. Elkaim and B. Parkinson. 1996. Automatic steering of farm vehicles using GPS. Paper presented at the *3rd International Conference on Precision Agriculture*. Minneapolis, MN, June 23-26.
- Stombaugh, T. S. 1998. Automatic guidance of agricultural vehicles at higher speeds. Ph.D diss. Library, Univ. of Illinois at Urbana-Champaign, IL.

## LIST OF SYMBOLS

$\Psi$	Vehicle yaw angle (deg)
$\alpha_r$	Front wheel turning ratio (ratio of steering rate to tractor speed) (rad/m)
$\delta$	Steering wheel angle (deg)
$C_{sf}$	Cornering stiffness of front wheels (N/rad)
$C_{sr}$	Cornering stiffness of rear wheels (N/rad)
$C$	Guidance controller transfer function
$c$	Numerator constant for vehicle transfer function
$D$	Steering controller transfer function
$d$	Distance of vehicle travel (m)
$d_s$	Distance along vehicle axis between position sensor and c.g. (m)
$e$	Lateral position error (m)
$F_x$	x coordinate of center of front axle (m)
$F_y$	y coordinate of center of front axle (m)
$G$	Steering actuator transfer function
$H$	Vehicle transfer function
$h$	Length along vehicle axis between front wheel and implement (m)
$l_x$	x coordinate of implement position (m)
$l_y$	y coordinate of implement position (m)
$I_{zz}$	yaw moment of inertia ( $\text{kg m}^2$ )
$K$	Feedback gain
$k$	discrete time step indicator
$L$	Wheel base (m)
$L_1$	Distance from c.g. to front axle (m)
$L_2$	Distance from c.g. to rear axle (m)
$m$	Vehicle mass (kg)
$s$	Laplace operator
$u$	control input
$V$	Vehicle forward velocity (m/s)
$y$	Recorded lateral position of vehicle (m)

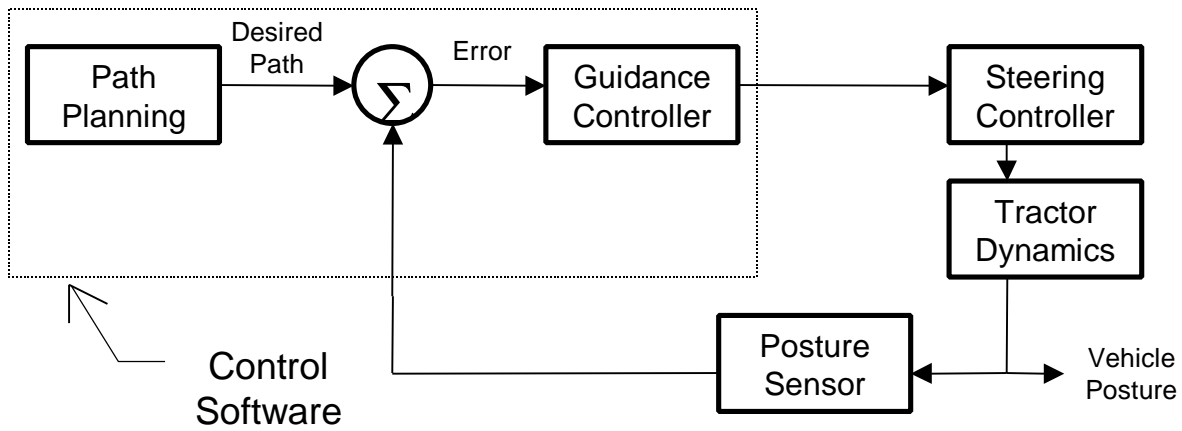


Figure 1. Signal flow diagram for an automatic vehicle guidance system.

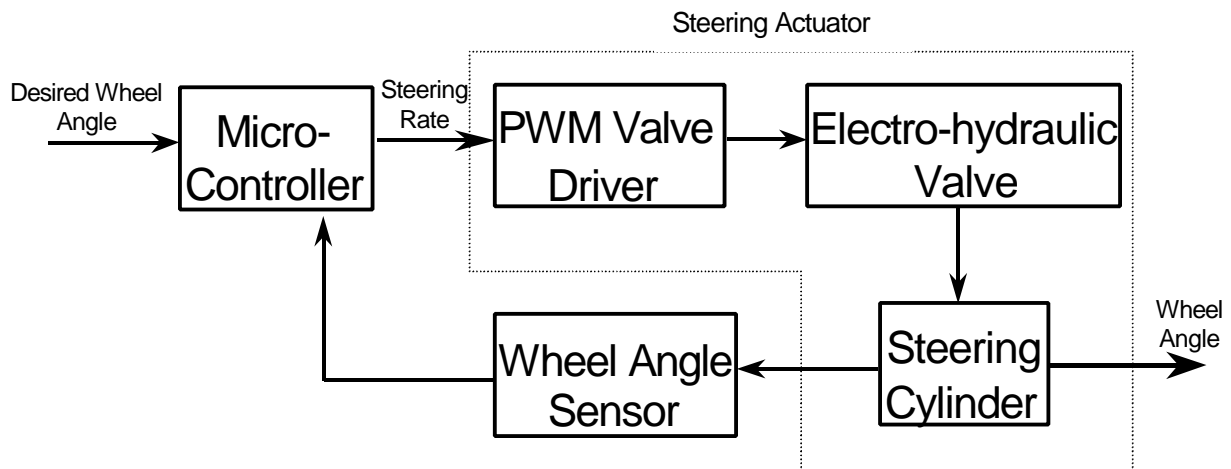


Figure 2. Steering controller configuration.

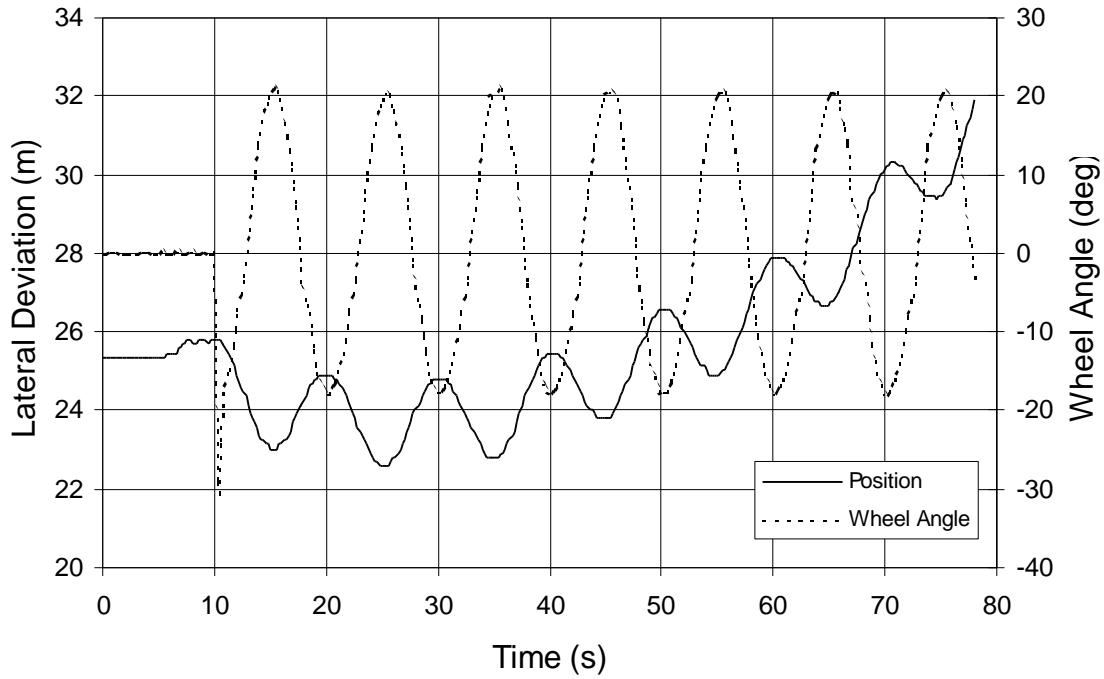


Figure 3. Measured wheel angle and vehicle lateral position as functions of time for a 0.1 Hz open loop frequency response test.

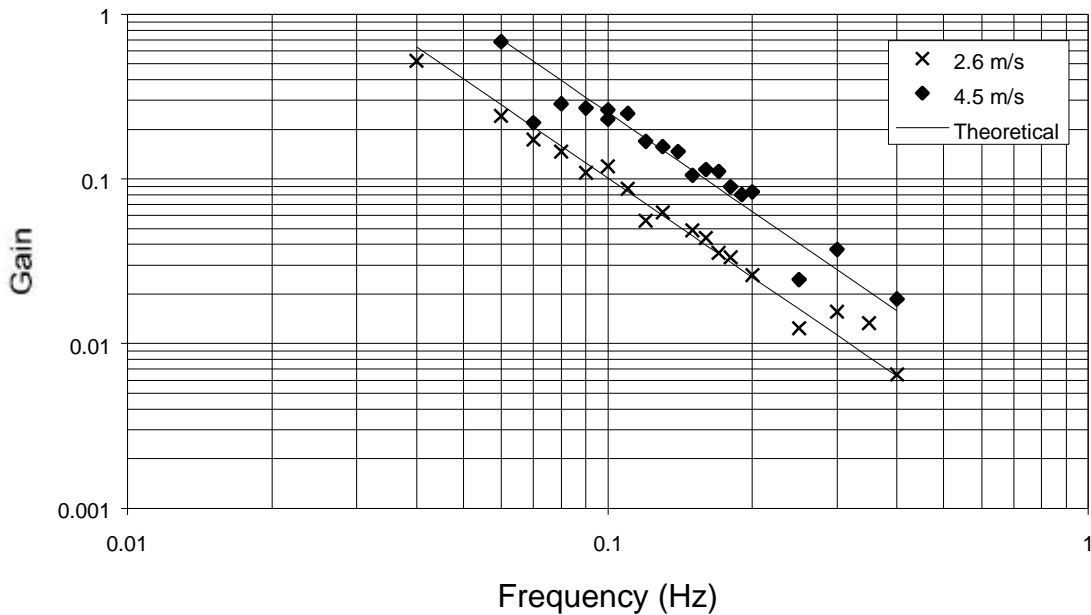


Figure 4. Open loop vehicle frequency response and theoretical model for two forward speeds.

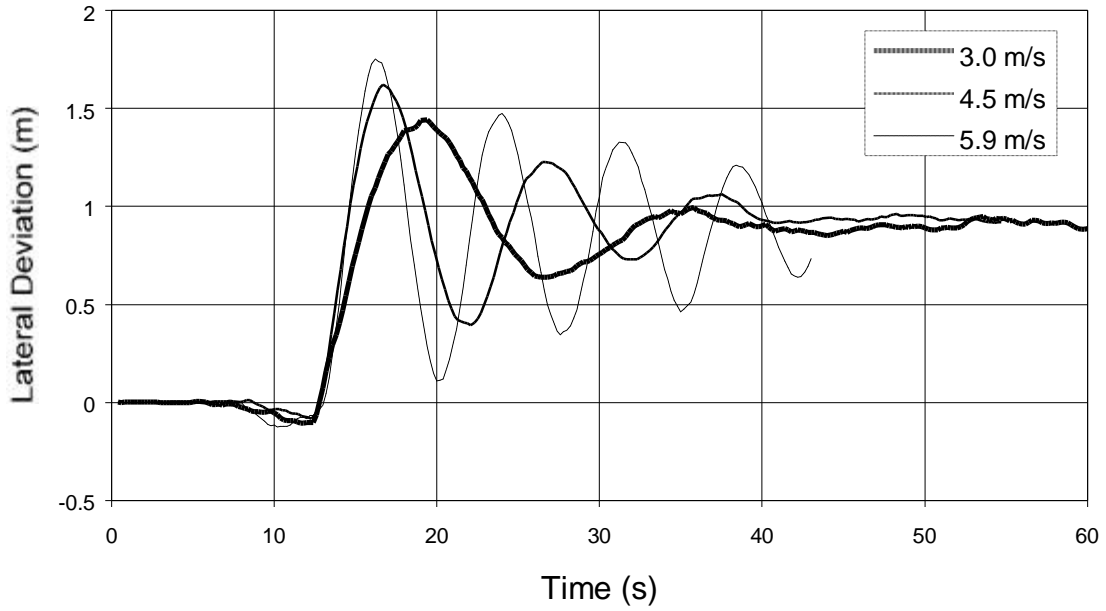


Figure 5. Unit step response of vehicle with preliminary guidance controller.

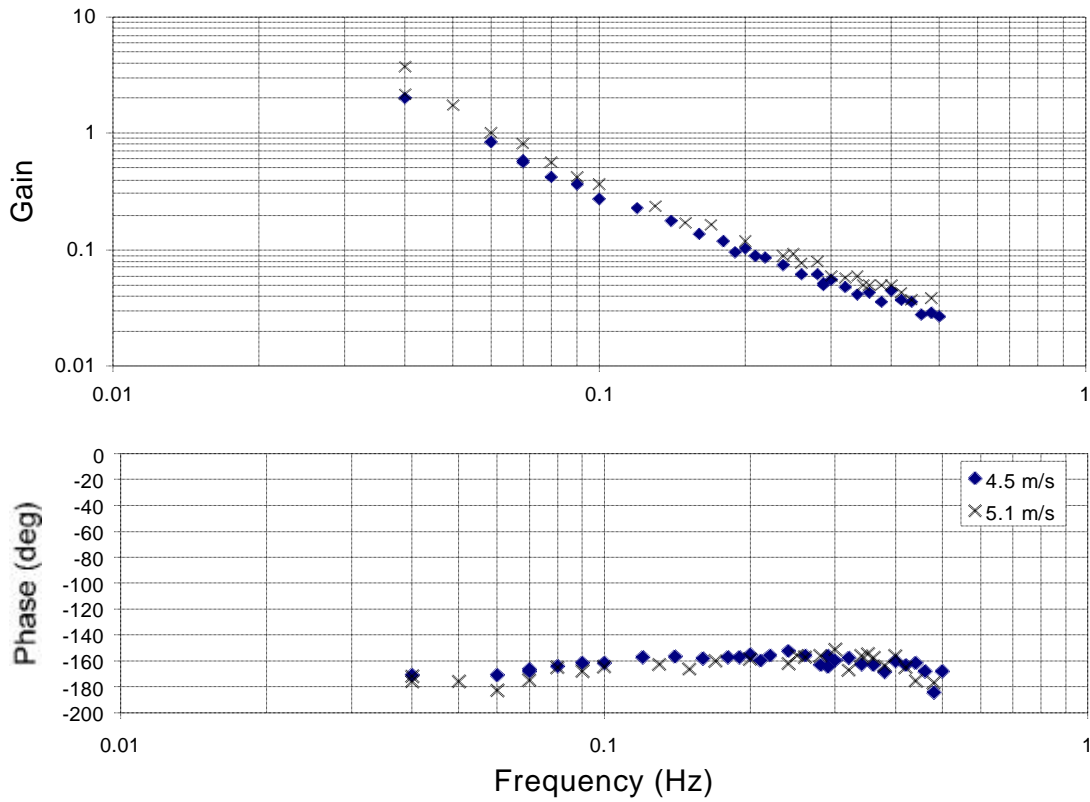


Figure 6. Bode plots of closed loop vehicle frequency response results.

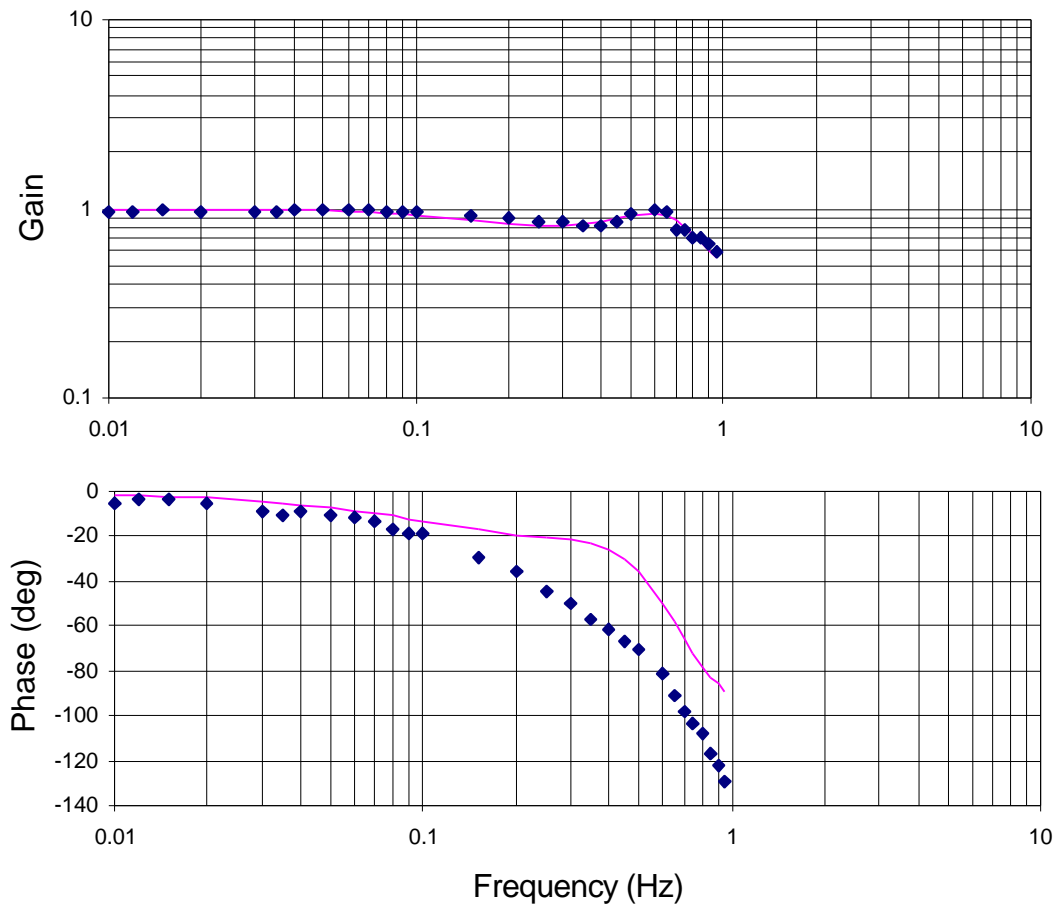


Figure 7. Bode plots of steering controller frequency response and a theoretical model of the response.

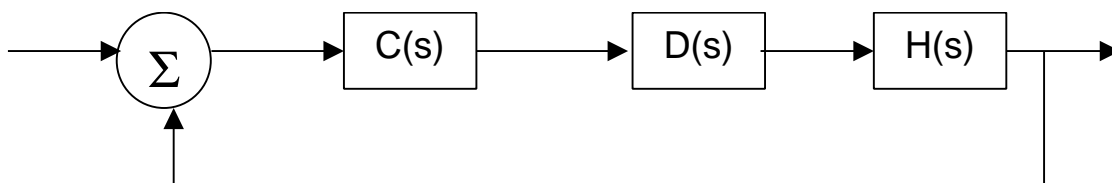


Figure 8. Guidance system block diagram including steering controller dynamics.

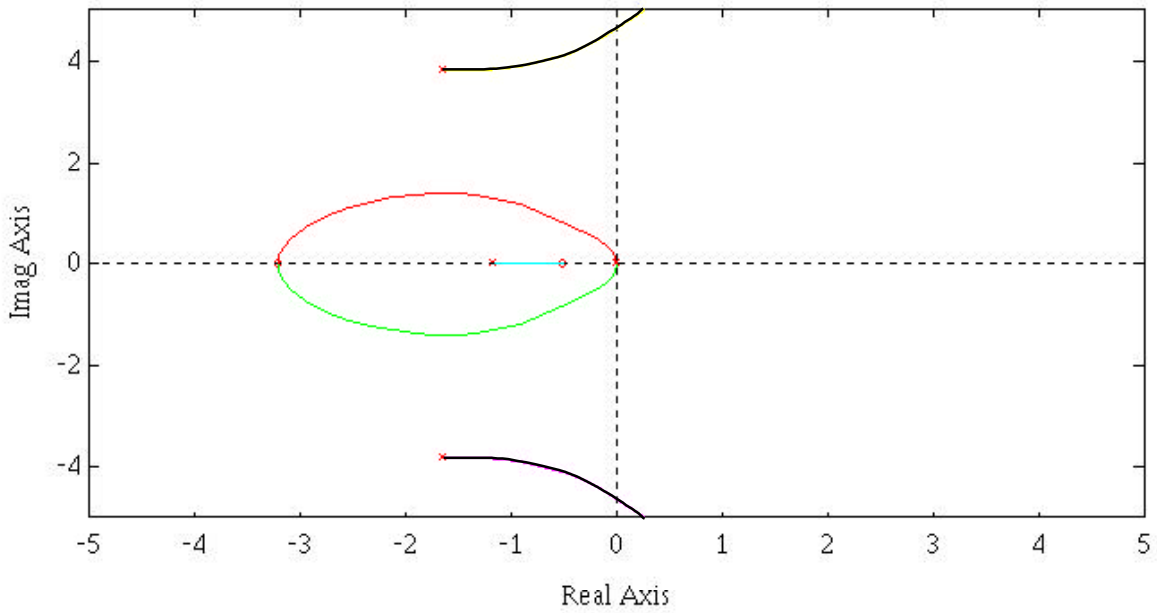


Figure 9. Partial root locus of vehicle, steering controller and guidance controller dynamics.

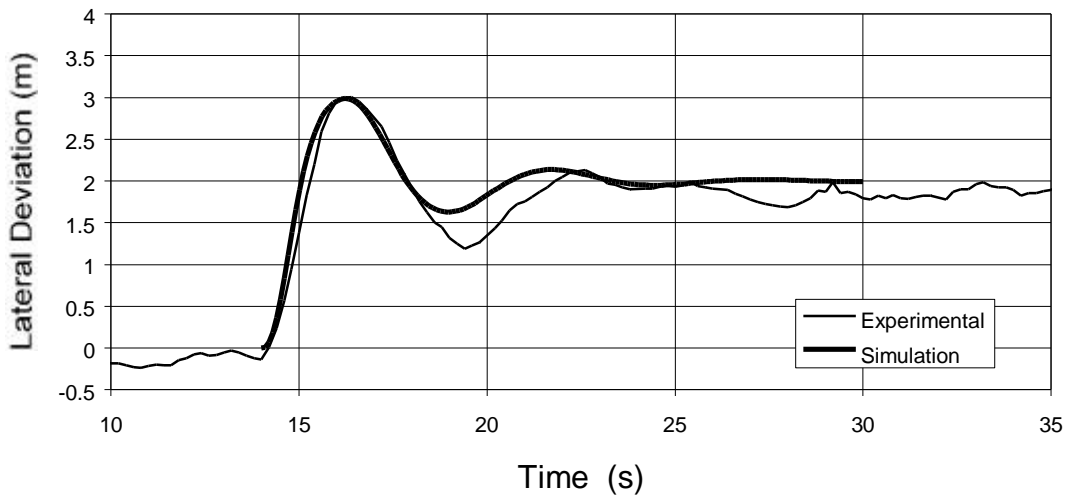


Figure 10. Comparison of experimental 2 m step response data at 3.9 m/s to simulation results that considered steering controller dynamics.

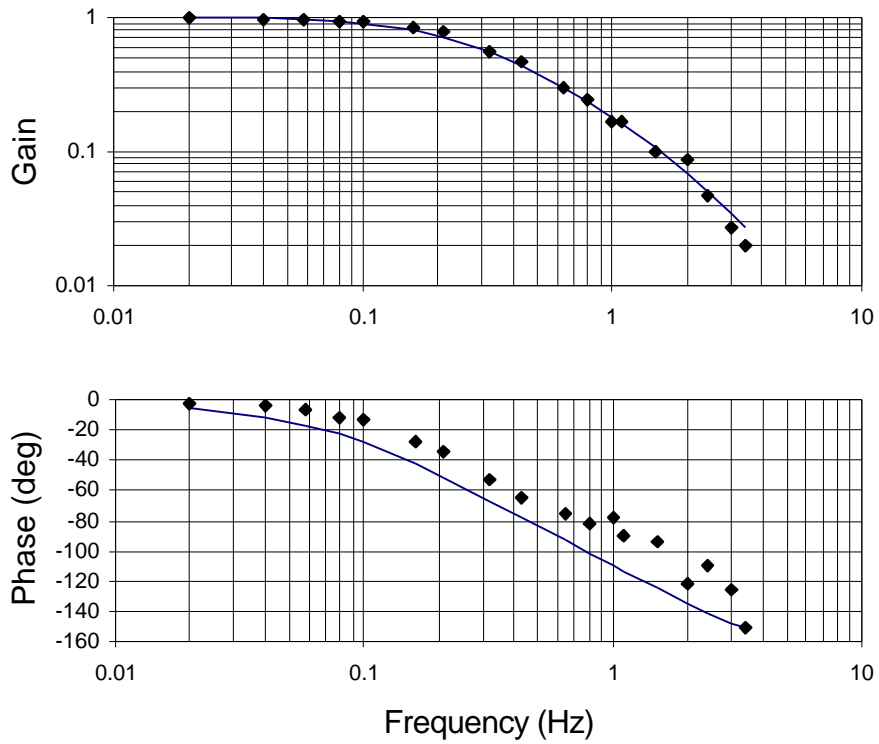


Figure 11. Frequency response of closed loop steering controller and theoretical second-order model.

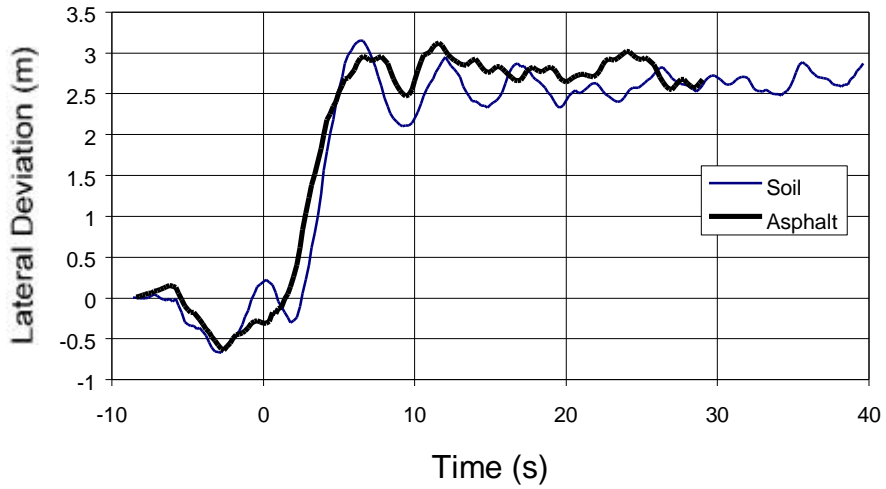


Figure 12. Three-meter step response of vehicle with open loop steering actuator at 4.5 m/s on soil and asphalt surfaces.

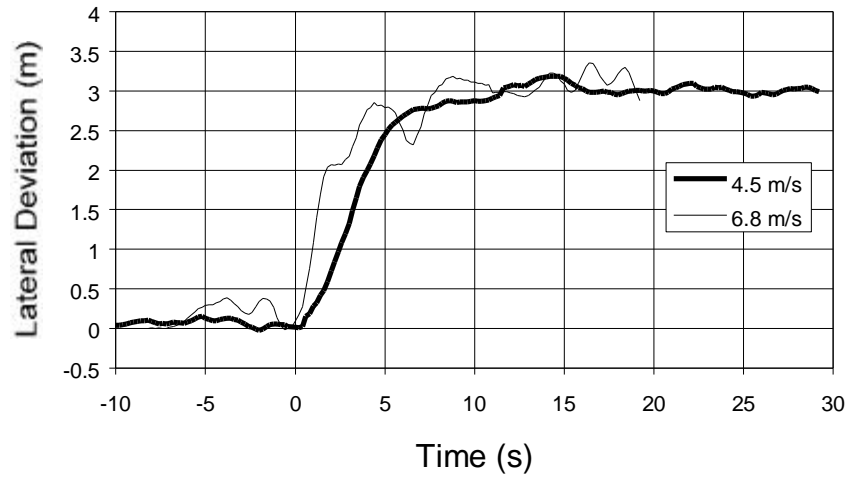


Figure 13. Three-meter step response of vehicle with open loop steering actuator after refinement of steering valve dead band compensation.

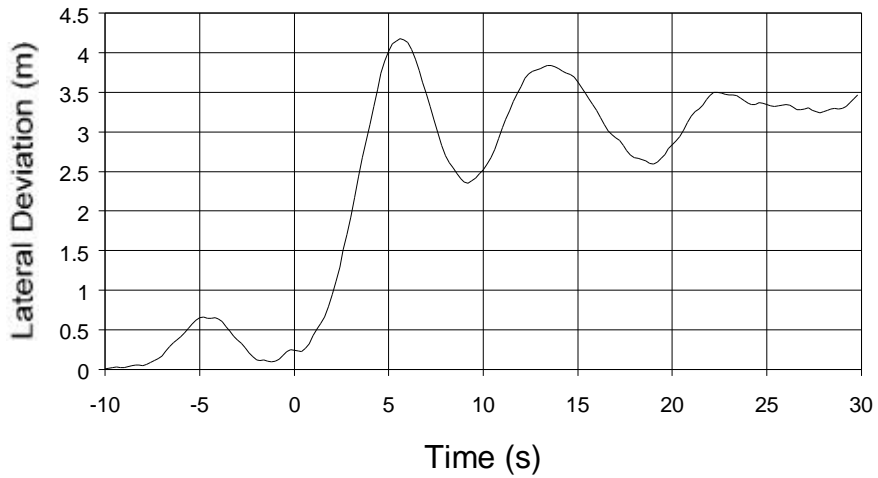


Figure 14. Three-meter step response of vehicle at 4.5 m/s with steering rate-based controller, sensor mounted over c.g. and position data integrated.